Electron paramagnetic resonance of magnetoelectric $Pb(Fe_{1/2}Nb_{1/2})O_3$

R. Blinc,[a] P. Cevc, A. Zorko, J. Holc, and M. Kosec
Jožef Stefan Institute, 1000 Ljubljana, Slovenia

Z. Trontelj and J. Pirnat
Institute for Mathematics, Physics and Mechanics, 1000 Ljubljana, Slovenia

N. Dalal, V. Ramachandran, and J. Krzystek
Florida State University, Tallahassee, Florida 32306

(Received 2 August 2006; accepted 20 November 2006; published online 1 February 2007)

To check on the nature of the weak magnetic order in polycrystalline magnetoelectric $Pb(Fe_{1/2}Nb_{1/2})O_3$ the *X*-band, *Q*-band, and far infrared electron paramagnetic resonance (EPR) spectra have been measured between 4 and 600 K and compared with magnetic susceptibility and magnetization data. The asymmetric line shapes can be simulated at higher temperature by thermally fluctuating superparamagnetic nanoclusters. The pronounced temperature dependence of the position of the spectra demonstrates the presence of an internal magnetic field which is small but nonzero even at room temperature, i.e., far above the antiferromagnetic transition. The electronic spin-spin exchange has been found to be in the terahertz range. The magnetization data reveal a weak ferromagnetism even above 300 K and a break in the temperature dependence of susceptibility at the paramagnetic to ferromagnetic transition. © *2007 American Institute of Physics*.
[DOI: 10.1063/1.2432309]

I. INTRODUCTION

Materials where long-range electric and magnetic orderings coexist[1] are of great interest for electronic devices as well as basic physics.[1–3] The possibility of electric field control of magnetism and magnetic field control of the electrical polarization is particularly challenging.[1–5]

The linear magnetoelectric (ME) effect is characterized by an axial second rank tensor Q_{ij} which is nonzero in 58 magnetic crystal classes. In the case of the magnetic point group $3m$ one has

$$M_1 = Q_{11}E_1, \tag{1a}$$

$$M_2 = Q_{11}E_2, \tag{1b}$$

$$M_{33} = Q_{33}E_3, \tag{1c}$$

so that the magnetoelectric effect is characterized by just two coefficients

$$a_{\parallel} = 4\pi Q_{11} \tag{2}$$

and

$$a_{\perp} = 4\pi Q_{33}. \tag{3}$$

Here $a_{\parallel}$ and $a_{\perp}$ refer to the directions parallel and perpendicular to the threefold crystal axis.

The magnetoelectric coupling may occur as a direct effect, i.e., as a linear coupling, $\mathbf{P}\cdot\mathbf{M}$, between the electric and magnetic order parameters. It may also occur as an indirect effect via the strain where the inclusion of the magnetostriction and/or piezomagnetism on one side and piezoelectricity and electrostriction on the other side produces cross terms between the polarization and the magnetization of the form P^2M^2. It is this indirect coupling which has been suggested to be responsible for the magnetoelectric effects in lead iron niobate $Pb(Fe_{1/2}Nb_{1/2})O_3$, abbreviated as PFN.[6] A linear ME effect at low temperatures was reported to occur in PFN by Watanabe and Kohn.[7] The exact nature of the ME coupling in PFN is thus still open and requires further studies.

PFN is a system where ferroelectric and magnetic orderings coexist below the Néel temperature. The ferroelectric phase transition takes place in a single crystal[6] around $T_c = 370-380$ K and the long-range antiferromagnetically ordered (AFM) phase begins below $T_N = 145$ K.[6,8–10] PFN is thus a ferroelectromagnet below $T_N = 145$ K. Anomalies in the dielectric properties have been reported[9] at T_N, demonstrating the existence of magnetoelectric coupling. Such a coupling is possible if both time reversal symmetry and spatial inversion symmetry are broken.[1] Recent single crystal studies have confirmed the existence of a jump of the dielectric constant at T_N as well as the changes in the dielectric constant induced by an applied magnetic field.[6,10] Above 380 K PFN is reported[9] to show relaxor ferroelectricity before it becomes pseudocubic above 400 K. Below 400 K the structure is rhombohedral,[11] $R3m$, with $a=b=c=4.058$ Å and $\alpha=\beta=\gamma=89.89°$. Whereas the PFN single crystal is rhombohedral it has been recently reported that PFN powder calcined at 1173 K exhibits a monoclinic perovskite phase.[12]

Very recently another dielectric anomaly has been observed around 20 K and a magnetic anomaly indicating an AFM-ferromagnetic transition around 10 K.[13] It should be mentioned that T_c as well as T_N and the low temperature anomalies are to a certain extent sample dependent and T_c varies in the interval between 300 and 380 K. In spite of the variation of T_c the same basic phenomena were found in all the investigated samples. Sol-gel derived PFN sintered ce-

[a]Electronic mail: robert.blinc@ijs.si

ramics shows ferroelectricity and weak ferromagnetism even at room temperature.[12] Relaxor properties have been observed in the magnetoelectric solid solution 0.8 $Pb(Fe_{1/2}Nb_{1/2})O_3$–0.2 $Pb(Mg_{1/2}W_{1/2})O_3$ abbreviated as PFN-PMW.[14,15]

At room temperature a regular pattern of dielectric domains, 20 nm in width and 20–50 nm in length, was identified with a scanning tip microwave near field microscope (STMNM).[11]

Mössbauer ^{57}Fe studies[6,10,11] of polycrystalline PFN showed a nonzero electric quadrupole doublet splitting, demonstrating that the Fe and Nb ions occupy noncubic off-center sites and are randomly disordered around the *B* sites of the perovskite octahedra. The Fe ions, in particular, are in a high spin state and the directions of the magnetic moments seem to be randomly distributed above 150 K in the absence of a magnetic field.[11]

The ^{57}Fe Mössbauer spectra also showed no magnetic sextet splitting above 300 K, implying that there are no significant internal magnetic fields above room temperature.[6,10,11] Below 80 K a sextet magnetic splitting does take place demonstrating the existence of magnetic order.[6] In has been further reported that the relation between the magnetization and the temperature below T_N is not the usual antiferromagnetic one.[8] The magnetization continuously increases below T_N with decreasing temperature, suggesting the existence of weak ferromagnetic order. The magnetic ordering around the trivalent iron ions may thus differ at different ionic sites, perhaps due to differences in superexchange with Ni^{5+} and oxygen.

Here we report on an electron paramagnetic resonance (EPR) study of polycrystalline PFN. *X*-band and *Q*-band spectra were studied as well as high-frequency EPR spectra at 381 and 683 GHz. In contrast to the case of ceramic samples the polycrystalline spectra were not Dyson-like, thus showing the absence of significant conductivity effects. We also measured the field cooled (FC) and zero field cooled (ZFC) magnetic susceptibilities as well as the magnetic hysteresis curves by a superconducting quantum interference device (SQUID) magnetometer between 2 and 390 K.

We particularly wished to study the magnetic order at the microstructural level and to compare the microscopic results with macroscopic susceptibility and magnetization data. This aspect is important to understand the nature of the magnetoelectric coupling in this system. We also wished to see whether the ferroelectric transition around 370–385 K affects the magnetic susceptibility. In addition we checked on the possible existence of small local magnetic fields induced by ferroelectric or relaxor order above the AFM transition at T_N=145 K, i.e., in a region where macroscopic magnetic order should be absent.

II. EXPERIMENT

$Pb(Fe_{0.5}Nb_{0.5})O_3$ (PFN) polycrystalline powder was prepared by mechanochemical synthesis.[16] The starting materials were powders of PbO (Aldrich 99.9+%), Fe_2O_3 (Ventron 99.9%), and Nb_2O_5. Synthesis was accomplished in air, in a Retsch PM 400 planetary mill working at 300 rpm. Tungsten carbide (WC) milling jar and balls with a powder/ball mass ratio of 1/5 were used. A batch of 200 g of powder was prepared. A deagglomeration treatment was accomplished for the synthesized powder by attrition milling in isopropanol for 4 h.

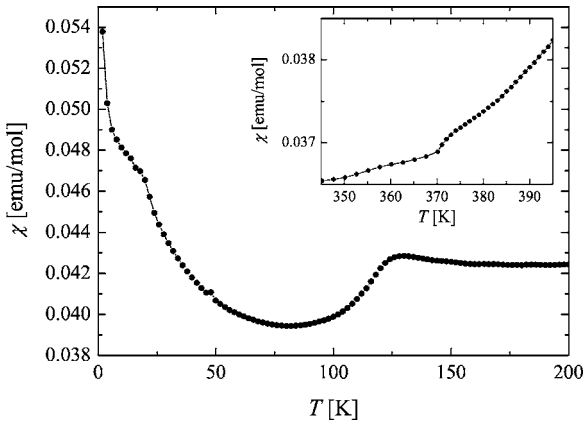

FIG. 1. Temperature dependence of the static dc magnetic susceptibility of PFN powder measured by a SQUID magnetometer at 200 G. The drop below 140 K is characteristic for the onset of antiferromagnetism. The insert shows the temperature dependence of the magnetic susceptibility around the ferroelectric transition temperature T_c=370 K.

Magnetic susceptibility and hysteresis measurements were performed on a Quantum Design SQUID magnetometer. The *X*-band and *Q*-band EPR spectra of polycrystalline PFN were studied on a Bruker spectrometer as a function of temperature between 600 and 4 K. High-frequency EPR spectra in the far infrared (381 and 683 GHz) region were obtained using the spectrometers[17,18] available at the National High Magnetic Field Laboratory in Tallahassee, FL. The onset of the ferroelectric transition was checked by dielectric measurements on pressed powder pellets.

III. EPR SPECTRA AND MAGNETIC SUSCEPTIBILITY

The dc magnetic susceptibility of PFN powder measured by a SQUID between 200 and 4 K at 200 G is shown in Fig. 1. The magnetic susceptibility slightly increases with decreasing temperature between 200 and 125 K and then drops between 125 and 60 K as expected for antiferromagnetic systems. Below 60 K the magnetic susceptibility starts to increase again with decreasing temperature. It shows a shoulder around 20 K and a very sharp increase below 10 K, demonstrating an AFM-ferromagnetic transition. It is important to note that the magnetic susceptibility shows a clear anomaly on going through the ferroelectric transition temperature around T_c=370 K (insert of Fig. 1). This seems to be a sign of a magnetoelectric effect.[2,7,8,19]

The *X*-band EPR spectra of polycrystalline PFN at 580, 292, 100, and 4 K are presented in Fig. 2. The solid lines correspond to theoretical fits described in Sec. IV. The *Q*-band spectra of PFN between 10 and 295 K are shown in Fig. 3. In both cases the spectra are *T* dependent. At 580 K the effective *g* factor is around 2.00. The spectra are slightly asymmetric. No new features are seen in the high-frequency

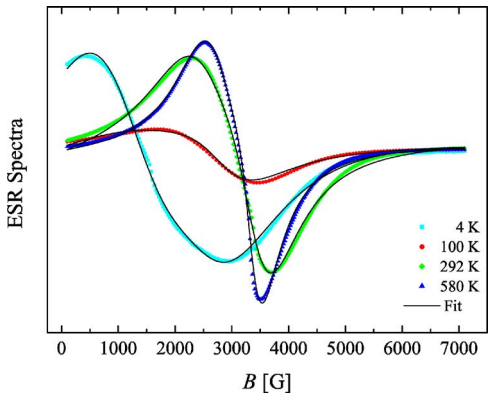

FIG. 2. (Color online) *X*-band EPR spectra of polycrystalline PFN at different temperatures. The solid lines correspond to theoretical fits to a model of thermally fluctuating superparamagnetic clusters, as described in Refs. 20 and 21. The nanocluster size amounts to 5–6 nm at room temperature.

spectra at 338 and 683 GHz (insert of Fig. 3), demonstrating that the EPR signal of PFN is from Fe^{3+} and there is no other oxidation state of Fe in the sample.

The temperature dependence of the shifts of the position of the EPR spectra is shown in Fig. 4 for the *X*-band data. The position of the center of gravity of the *X*-band spectra between 600 and 480 K is at first nearly *T* independent and then starts to move to higher fields with decreasing temperature. Below 480 K it starts to move to lower fields with decreasing temperature. There are breaks in the shift versus *T* curve around 450 K, i.e., at the onset of the relaxorlike phase, and around T_c where the ferroelectric phase starts. Most pronounced is the change of slope around 120–145 K, i.e., at the onset of the AFM phase. The *X*-band shifts above 120 K are relatively small and amount to 100–200 G. In the AFM phase below 120 K the shift to lower fields becomes quite large and reaches 1600 G at low temperatures. It should be mentioned that the position of the center of the line does not depend on the history and direction of the temperature variation above 130 K. Below this temperature slight hysteresis effects were observed.

The width of the spectra is quite large (Fig. 5). There is practically no difference between the width of the *X*-band and the *Q*-band spectra. The peak-to-peak width is nearly temperature independent between 600 and 450 K and

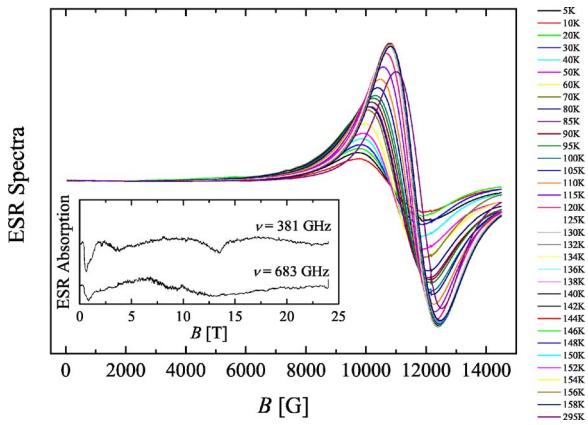

FIG. 3. (Color online) *Q*-band EPR spectra of polycrystalline PFN between 10 and 295 K. The temperature is increased from 10 K up.

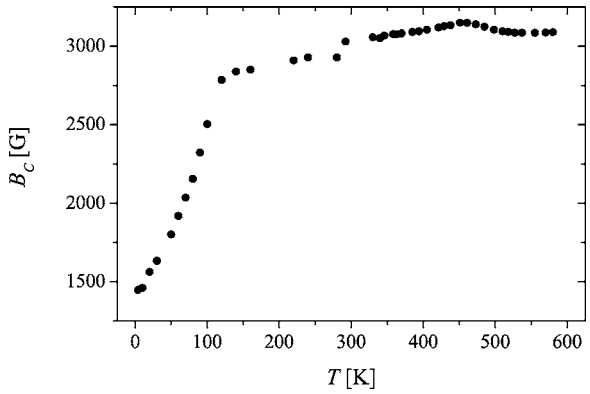

FIG. 4. Shift of the center of the gravity of the *X*-band EPR spectra as a function of temperature.

amounts to more than 1500 G. There is a clear change in the slope at 450 K, i.e., at the same temperature where a change in the slope was also seen in the *T* dependence of the position of the center of the line and where the system (according to the x-ray data) becomes noncubic. At the transition to the ferroelectric phase, which takes place in this particular sample around 300 K, there is another change in the slope. The most pronounced change in the *T* dependence of the width occurs at the transition to the antiferromagnetic phase below 120 K. The broadening seems to follow the *T* dependence of the AFM sublattice magnetization as indeed expected for a powder sample. There is another significant change in the slope around 10 K where another magnetic transition seems to take place. At low temperatures the peak-to-peak width reaches approximately 4000 G. The spectra are not Lorentzian and are slightly asymmetric even at room temperature.

It should be stressed that the *T* dependences of the width of the spectra and the shift of centers of gravity to lower fields (effective internal fields) are practically identical (Fig. 5) in the *Q* band and in the *X* band. This shows that the widths of the spectra are not determined by the external magnetic field B_0 as in the case of *g*-tensor anisotropy.

IV. DISCUSSION

The presence of a small but nonzero internal magnetic field deduced from the EPR spectra even at temperatures above the AFM phase is puzzling and requires comparison with the magnetization data.

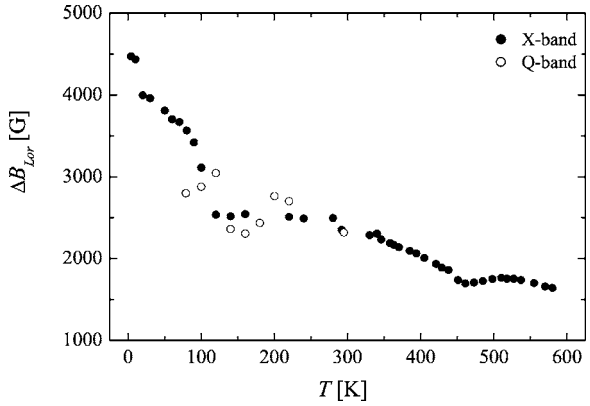

FIG. 5. The widths of the *X*-band (full dots) and *Q*-band (empty dots) EPR spectra as a function of temperature.

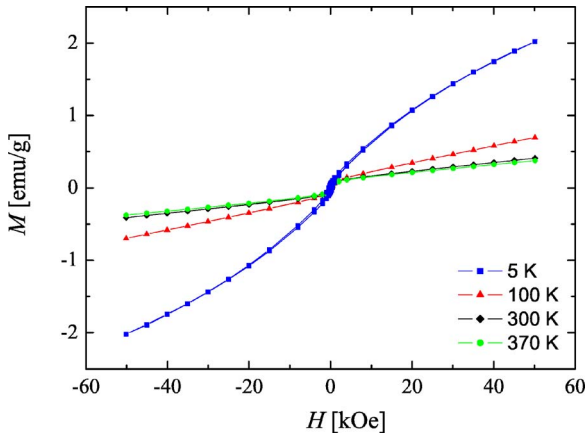

FIG. 6. (Color online) Magnetic field dependence of the magnetization at various temperatures. The nonlinear behavior of the magnetization vs magnetic field plots persists to 370 K, demonstrating the existence of weak ferromagnetism.

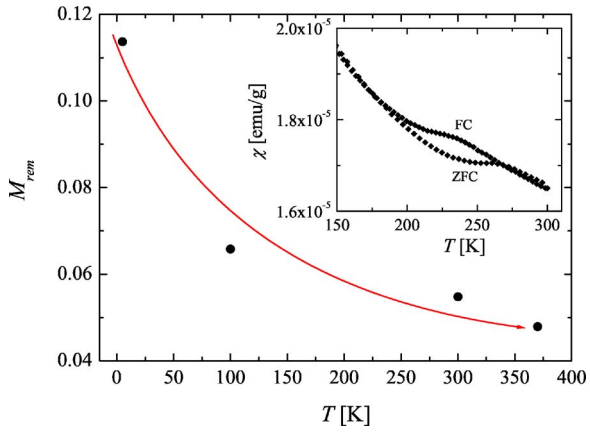

FIG. 8. (Color online) Temperature dependence of the remanent magnetization in PFN powder. The insert shows the difference between the FC and ZFC static magnetic susceptibilities above T_N, demonstrating the existence of a nonequilibrium state, which disappears in the antiferromagnetic phase.

The magnetic field dependence of the magnetization of polycrystalline PFN has been measured between −50 and 50 kOe (Fig. 6). It is nonlinear at all temperatures between 5 and 370 K. The corresponding hysteresis curves are shown in Fig. 7 for fields between −2 and 2 kOe at 5, 100, 300, and 370 K. The important point to note is that over the whole investigated temperature range, i.e., in the AFM phase and the ferroelectric phase, the remanent magnetization is nonzero, though small.

The T dependence of the remanent magnetization M_R is presented in Fig. 8. M_{rem} changes from 0.11 emu/g at 5 K to 0.07 emu/g at 100 K and ≈0.05 emu/g at 300 and at 370 K and shows no tendency to vanish with increasing temperature. This is similar to the quadrupolar splitting in the Mössbauer spectra[11] which is as well nearly T independent between 150 and 300 K. It is also similar to the EPR data which show a nonvanishing internal field up to 400 K.

It should be noted that the observed slightly asymmetric EPR line shapes above room temperature (Fig. 2) can be simulated[20,21] by a model involving the presence of thermally fluctuating superparamagneticlike nanoclusters (insert of Fig. 2). Above room temperature the effective volume of these nanoclusters corresponds to a dimension of 5–6 nm. It thus seems that we indeed deal in PFN with magnetoelectric nanoclusters at room temperature.

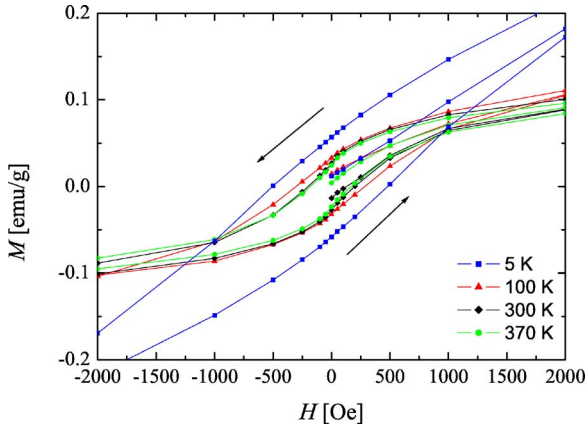

FIG. 7. (Color online) The "slim" magnetization hysteresis curves of PFN at different temperatures.

The finite-though small magnetizations and the resulting internal fields above T_N seem to reflect the existence of magnetoelectric coupling. This might be either indirect[19] via piezomagnetism and/or magnetostriction and piezoelectricity and electrostriction or direct via the coupling of the local polarizations and magnetizations in superparamagnetic polar nanoclusters in the paraelectric and ferroelectric phases of disordered PFN. The local symmetry of these clusters is, namely, much lower than the macroscopic symmetry. Both time reversal and space reversal symmetries could well be broken when the clusters freeze out or coalesce into macroscopic static domains in the ferroelectric phase, so that both the direct and the indirect coupling could take place. The exact nature of the magnetoelectric effect is still open but it should be stressed that both above mechanisms, the direct and the indirect one, are allowed by symmetry in PFN below T_N. The existence of a small but nonzero magnetoelectric effect is also supported by the observation of a clear anomaly in the magnetic susceptibility on going through the ferroelectric transition temperature (insert of Fig. 1). The fact that we deal in PFN with weak ferromagnetism up to 370 K, which is superimposed on the AFM order below T_N, is also supported by the difference between the static FC and ZFC magnetic susceptibilities between 275 and 150 K, i.e., above the AFM transition at T_N (insert of Fig. 8). Such a difference is characteristic for nonergodic systems with pinned domain walls or relaxorlike systems. It disappears in the long-range ordered magnetic phase if the external field is large enough (1 T) to depin the domain walls or clusters.

A weak magnetization in PFN ceramics and calcined powders has been indeed recently reported even at room temperature[12] supporting our conclusions.

V. CONCLUSIONS

EPR measurements on PFN over a wide frequency range (10–683 GHz) and temperature (4–600 K), combined with magnetization data, show first that the Fe ions are in the Fe^{3+}

oxidation state. Second, electronic spin-spin exchange is at least in the terahertz range, since the spectra are found to be single peaks (averaged over the various spin states of the $S=5/2$ state) at all temperatures and frequencies up to 683 GHz. Third, PFN is a multiferroic material where the electric and magnetic polarizations are coupled directly or indirectly not only on the macroscopic but apparently also on the local level. An especially important finding is the anomaly in the magnetization at the transition from the paraelectric phase to the ferroelectric phase. Additional measurements are needed to fully characterize this observation.

[1]G. A. Smolenskii and I. E. Chupis, Sov. Phys. Usp. **25**, 475 (1982) and references therein.
[2]M. Fiebig, J. Phys. D **38**, R123 (2005).
[3]D. L. Fox and J. F. Scott, J. Phys. C **10**, L329 (1977).
[4]S. Goshen, D. Mukamel, H. Shaked, and S. Shtrikman, J. Appl. Phys. **40**, 1590 (1969).
[5]G. A. Smolenskii, A. I. Agranovskya, S. V. Isupov, and V. A. Isupov, Sov. Phys. Tech. Phys. **3**, 1981 (1958).
[6]Y. Yang, J.-M. Liu, H. B. Huang, W. Q. Zou, P. Bao, and Z. G. Liu, Phys. Rev. B **70**, 132101 (2004).
[7]T. Watanabe and K. Kohn, Phase Transitions **15**, 57 (1989).
[8]V. V. Bhat, A. M. Umarji, V. B. Shenoy, and U. V. Waghmare, Phys. Rev. B **72**, 014104 (2005); V. A. Bokov, I. E. Mylnikov, and G. A. Smolenskii, Sov. Phys. JETP **42**, 643 (1961); I. E. Mylnikov, and G. A. Smolenskii, Sov. Phys. Usp. **15**, 447 (1992).
[9]X. S. Gao, X. Y. Chen, J. Vin, J. Wu, Z. G. Liu, and M. Wang, J. Mater. Sci. **35**, 5421 (2000).
[10]J. T. Wang, C. Zhang, Z. X. Shen, and Y. Feng, Ceram. Int. **30**, 1627 (2004).
[11]Y. Yang, S. T. Zhang, H. B. Huang, Y. F. Chen, Z. G. Liu, and J.-M. Liu, Mater. Lett. **59**, 1767 (2005).
[12]S. B. Majmuder, S. Bhattacharyya, and R. S. Katiyar, J. Appl. Phys. **99**, 024108 (2006).
[13]Z. Trontelj, Z. Jagličič, A. Levstik, C. Filipič, and M. Kosec (unpublished).
[14]H. Lee and W. K. Choo, J. Appl. Phys. **52**, 5767 (1981).
[15]A. Tawfik, M. I. Abd El-Ati, and M. M. Abou-Sekkina, J. Phys. Soc. Jpn. **54**, 2730 (1985).
[16]D. Kuščer, A. Meden, J. Holc, and M. Kosec, J. Am. Ceram. Soc. (to be published).
[17]B. Cage, A. Hasan, L. Pardi, J. Krzystek, L. C. Brunel, and N. S. Dalal, J. Magn. Reson. **124**, 495 (1997).
[18]S. A. Zvyagin, J. Krzystek, P. H. M. van Loosdrecht, G. Dhalenne, and A. Revcolevschi, Physica B **346–347**, 1 (2004).
[19]W. Eerenstein, N. D. Mathur, and J. F. Scott, Nature (London) **442**, 759 (2006).
[20]R. S. de Biasi and T. C. Devezas, J. Appl. Phys. **49**, 2466 (1978).
[21]R. Berger, J. Kliava, J. C. Bissey, and V. Baïetto, J. Phys.: Condens. Matter **10**, 8559 (1998); J. Kliava, J. C. Bissey, and V. Baïetto, J. Appl. Phys. **87**, 7389 (2000).